ISSN 1061-9348, Journal of Analytical Chemistry, 2016, Vol. 71, No. 3, pp. 276–282. © Pleiades Publishing, Ltd., 2016.

ARTICLES

Properties of Gold Electrode Modified with Dimercaptosuccinic Acid and Electrochemical Behavior of Copper Histidine Complex[1]

I. Kerekovic[a], * and K. Wittine[b], **

[a] Department of General and Inorganic chemistry, Faculty of Chemical Engineering and Technology, University of Zagreb
10000 Zagreb, Marulićev trg 19, Croatia
[b] Department of Biotechnology, University of Rijeka, 51000 Rijeka, Radmile Matejčić 2, Croatia
*e-mail: irena.kerekovic@fkit.hr
**e-mail: karlo.wittine@biotech.uniri.hr

Received July 2, 2014; in final form, June 29, 2015

Abstract—A self-assembled monolayer of *meso*-2,3-dimercaptosuccinic acid was prepared on the surface of gold disc electrode. The modified electrode was characterized using cyclic voltammetry in copper(II) solution and cyclic voltammetry and electrochemical impedance spectroscopy in the presence of potassium hexacyanoferrate(II)/(III) and hexaammineruthenium (II)/(III) chloride. Binding of copper(II) histidine complex (**Cu–His**) onto the electrode was successfully achieved for a wide range of tested concentrations, as shown with adsorption transfer stripping voltammetry. Electrode response ($\log\Delta I_p$) was linearly proportional to logc(Cu–His) with correlation coefficient $R^2 = 0.9839$.

Keywords: self-assembled monolayer, *meso*-2,3-dimercaptosuccinic acid, histidine, adsorption transfer stripping voltammetry

DOI: 10.1134/S1061934816030047

Nuzzo and Allara discovered self-assembled monolayers (**SAMs**) in 1983 [1], and since then thiol and disulfide SAMs on gold were the subject of numerous studies. SAMs represent an ideal approach to the transformation of physical and chemical properties of the surface, thereby providing an interface to developing new sensors, detectors and electronic components [2].

Histidine is an essential amino acid [3], constituent of many proteins. It plays an important role in physiological and metabolic processes [4]. Tendency of His to adsorb on gold presents a problem in electrochemical measurements with gold electrodes. It was found that His coordinates to gold through carboxylic group over one [5] or both [6] oxygens. Copper(II)–histidine complexes have been thoroughly investigated, and structure and charge of the complexes have been defined [7]. During the formation of Cu–His, the copper(II) cation can be attached to the carboxylic and amino group and the imidazole nitrogen atom of histidine forming monodentate [8], bidentate [9, 10] or tridentate [11] complexes. The formed bonds block the functional groups responsible for the adsorption of His on gold [5, 6]. The structure of the complex in aqueous solutions depends on the ratio of the metal ion to the ligand and pH [7]. For a 1 : 1 mole ratio at pH 6, the dominant structure is $[Cu(His)]^+$ [12]. Owing to the Jahn–Teller effect, Cu^{2+} forms stable complexes with organic ligands [13, 14]. Therefore, $[Cu(His)]^+$ has a capability for an additional complexation with carboxylic groups of bound *meso*-2,3-dimercaptosuccinic acid (**DMSA**), creating tetradentate or pentadentate coordination.

Electrochemical impedance spectroscopy (**EIS**) is a nondestructive powerful tool used to study and characterize modification of electrodes based on SAMs as well as many other fields of research such as corrosion, fuel cells and batteries, coatings, conductive polymers and analytical determination of inorganic and organic substances [15]. The fundamental advantage of EIS is equivalent circuit modeling of data in order to extract physically meaningful properties of the electrochemical system. Adsorption transfer stripping voltammetry (**AdTSV**) was used for the evaluation of Cu–His binding to modified electrode. AdTSV is a technique corresponding to the anodic and cathodic stripping voltammetry. The difference lies in the accumulation step that is not electrochemically controlled but accomplished during a process of adsorption. Adsorption and measurement steps are conducted in different solutions [16].

The purpose of this research was to study electrochemical behavior of Cu–His complex at *meso*-2,3-dimercaptosuccinic acid assembled on gold. The char-

---

[1] The article is published in the original.

acteristic of adsorbed DMSA was identified by examining electrochemical performance of two redox pairs, $Fe(CN)_6^{3-/4-}$ and $Ru(NH_3)_3^{3+/2+}$ with cyclic voltammetry (**CV**) and EIS. The possibility of employing modified electrode as a recognition element for indirect detection of histidine was investigated with AdTSV.

EXPERIMENTAL

Reagents. *meso*-2,3-Dimercaptosuccinic acid was obtained from Acros Organics. Acetic acid, sodium acetate, sodium perchlorate, ethanol for DMSA preparation, potassium hexacyanoferrate(II) and ethylenediaminetetraacetic acid (**EDTA**) for electrode recovery were from Kemika. Histidine, hexaammineruthenium(III) chloride and hexaammineruthenium(II) chloride were from Sigma–Aldrich. Potassium hexacyanoferrate(III) and perchloric acid were from Merck and copper(II) nitrate was from Alkaloid. A 0.1 M acetate buffer (**ACB**) with pH 4.6 containing 0.1 M sodium perchlorate was used. All the chemicals were of analytical grade and all solutions were prepared with water from Millipore MilliQ system (USA).

Instruments. A conventional three-electrode cell consisting of a modified electrode as working, $Hg|Hg_2Cl_2|KCl$ saturated as reference and platinum wire as counter electrode was used. CV measurements were performed at Potentiostat 264 A (Princeton Applied Research, USA) connected to a computer for data collecting and analysis using EG&G PowerSuite software. The applied potential scan rate in CV was 50 mV/s. Potentiostat/Galvanostat 263A (Princeton Applied Research, USA) combined with Frequency Response Detector 5210 (EG&G Instruments, PAR, USA) connected to a computer for data acquisition and analysis using EG&G PowerSuite software was used for EIS measurements. AC amplitude potential of ±5 mV was superimposed to DC potential (formal potential of redox couple) and frequency range between 100 mHz and 100 kHz was examined. Equivalent circuit parameters were calculated by fitting the EIS data using appropriate circuit by ZsimpWin software provided by EG&G. AdTSV measurements were carried out on a polarographic analyzer/stripping voltmeter 264A (Princeton Applied Research, USA) connected to a computer for data acquisition with E-Corder 410 using Chart & Scope software. Spectrometric measurements were performed using a spectrophotometer DMSA-80 (Varian, USA). All potentials in this work are given versus the reference electrode. All solutions were deaerated with nitrogen gas for 10 min before measurements and experiments were performed at room temperature.

Preparation of Au/DMSA electrode. The polycrystalline working gold electrode of 1 mm diameter was polished to a mirror-like surface with 1 μm and then 0.25 μm Al_2O_3 powder. Afterwards the electrode was ultrasonically cleaned in ultra pure water (5 min), immersed in Piranha solution (5 min) and rinsed with ethanol. Subsequently, the electrode was electrochemically polished in 0.1 M $HClO_4$ between 0 and 1.7 V until reproducible voltammograms were observed. Modification of a gold electrode was performed in 5 mM DMSA in ethanol for 48 h at the room temperature in the dark. After removal from DMSA solution, the electrode was thoroughly washed with ethanol to eliminate physically adsorbed species. The proposed schematic illustration of DMSA assembling to Au electrode and binding of Cu–His complex can be shown as follows:

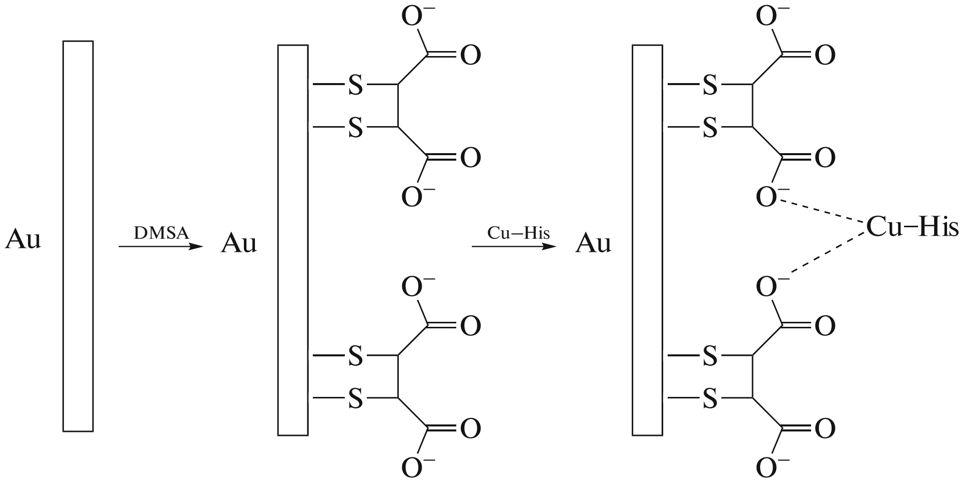

Preparation of Cu–His complex. In order to minimize the influence of nonspecific adsorption of His on Au, Cu–His complex was prepared by mixing 2 mL 0.1 M solution of Cu^{2+} with 2 mL of 0.1 M solution of

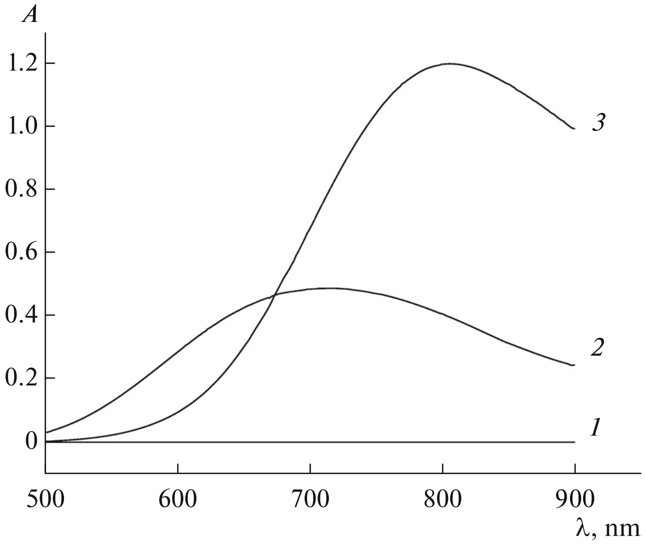

Fig. 1. Absorbance spectra of 0.1 M His (*1*), 0.02 M Cu–His complex (*2*) and 0.1 M Cu^{2+} (*3*), 100 nm/min.

His at pH 6 and dilution with deionized water to a volume of 10 mL. Complex formation was indentified spectrophotometrically. Figure 1 illustrates the spectra recorded for His, Cu^{2+}, and Cu–His. His has no visible absorption maximum in the investigated spectral region. Hydrated Cu^{2+} has a maximum absorbance at approximately 800 nm, while the Cu–His has a maximum absorbance slightly below 700 nm, which is in good agreement with theory [17]. Decrease in the absorption intensity of Cu–His compared to Cu^{2+} was the result of five times lower concentration of the prepared complex in relation to Cu^{2+} cation.

RESULTS AND DISCUSSION

Electrochemical characterization of Au/DMSA electrode. Au/DMSA electrode was characterized with CV and EIS with positive and negative redox pairs. Comparing the electron transfer reactions of $Fe(CN)_6^{3-/4-}$ and $Ru(NH_3)_3^{3+/2+}$ on metal electrodes and SAM-modified surfaces, binding of organic molecules can be confirmed. Likewise we can demonstrate performance of the layer depending on the medium in which the measurement is carried out. Cyclic voltammograms were recorded in 0.1 M ACB containing 0.1 M $NaClO_4$, pH 4.6, with 1 mM $Fe(CN)_6^{3-/4-}$ and 1 mM $Ru(NH_3)_3^{3+/2+}$. In acidic solution (pH 4.6) carboxylic groups of DMSA are deprotonated, $pK_{a1} = 2.71$, $pK_{a2} = 3.43$ [18] and the surface becomes negatively charged. Therefore, reduction in measured peak current (I_p) and increase in peak-to-peak separation (ΔE_p), relatively a bare electrode, is expected for $Fe(CN)_6^{3-/4-}$ due to electrostatic repulsion between the negatively charged electrode surface and negative redox pair [19] (Fig. 2a). $Fe(CN)_6^{3-/4-}$ on Au electrode exhibited ΔE_p of ~67 mV, indicating a reversible electrochemical reaction [20]. Subsequent to DMSA binding, an increase in ΔE_p (~100 mV) and decrease in I_p (~0.3 μA) were observed. DMSA attached to Au blocked the surface and slowed the charge transfer reaction; consequently, reversible reaction became quasi-reversible. Given that the

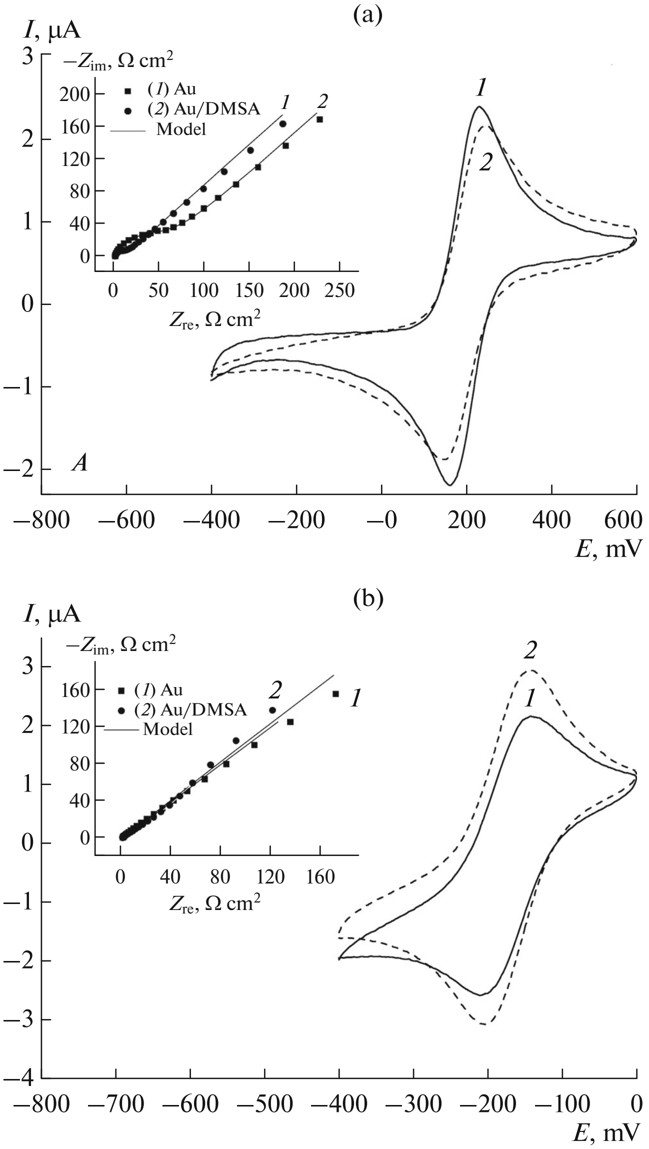

Fig. 2. Cyclic voltammograms recorded in 0.1 M ACB containing 0.1 M $NaClO_4$, pH 4.6, with 1 mM $Fe(CN)_6^{3-/4-}$ (a) and 1 mM $Ru(NH_3)_3^{3+/2+}$ (b) on Au (solid line) (*1*) and Au/DMSA (dashed line) (*2*). Scan rate 50 mV/s. Insets: Nyquist plots recorded under the same conditions. Experimental data are shown as symbols, and calculated values as lines.

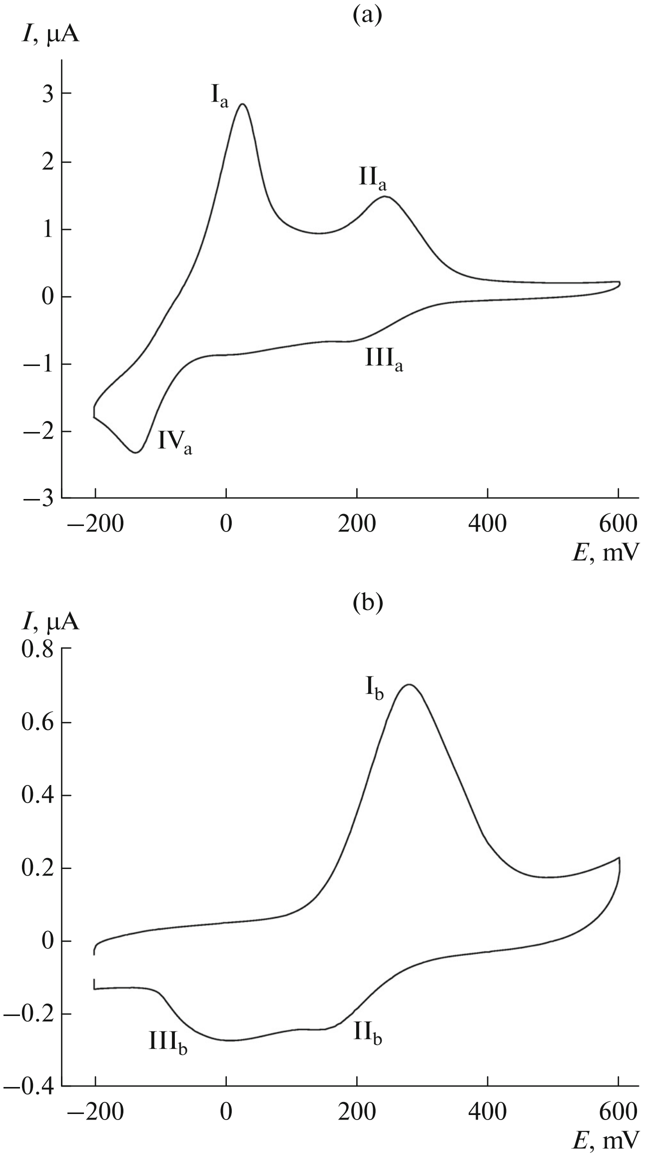

Fig. 3. Cyclic voltammograms of Au (a) and Au/DMSA (b) electrodes recorded in 0.1 M ACB containing 0.1 M $NaClO_4$, pH 4.6, with 0.1 M $Cu(NO_3)_2 \cdot 3H_2O$. Scan rate 50 mV/s.

charge transfer resistance increased, current peak was shifted and the time required to reach the top, at the same scan rate, was greater. As a result, the thickness of the diffusion layer increased, so the diffusion rate reduced. These observations are in agreement with those obtained for the microelectrode and suggest that the electron transfer reactions occur at pinholes in the SAMs [21, 22].

Likewise, $Ru(NH_3)_3^{3+/2+}$ illustrated reversible electrochemical response (ΔE_p ~ 67 mV) on Au electrode. Following binding of DMSA, an increase in I_p (~0.8 μA) and decrease in ΔE_p were observed (Fig. 2b). Anticipated growth of I_p and decline in ΔE_p (ΔE_p ~57 mV) can be attributed to electrostatic attraction between negatively charged electrode surface and positive redox pair. The impedance data was approximated using Randles equivalent circuit with CPE element [23]. The circuit includes electrolyte solution resistance (R_s) which represents properties of electrolyte solution and geometry of the system and Warburg impedance (Z_w) which stands for impedance, caused by the diffusion of the redox probe. Both R_s and Z_w should not be affected by modification of the surface [24]. Charge transfer resistance (R_{ct}) and double layer capacitance (C_{dl}) are parameters that are connected to the dielectric and insulating properties at the electrode/electrolyte interface; therefore, they are influenced by managing the electrode surface [24]. Impedance measurements were performed in 0.1 M ACB containing 0.1 M $NaClO_4$, pH 4.6, with 1 mM $Fe(CN)_6^{3-/4-}$ and 1 mM $Ru(NH_3)_3^{3+/2+}$. Nyquist plot for Au recorded in solution containing $Fe(CN)_6^{3-/4-}$ demonstrated an almost straight line with weakly expressed semicircular segment, which is a response characteristic for a mass-transfer-limited process (Fig. 2a, inset). Comparing impedance plots of Au and Au/DMSA electrodes, one could see that adsorbed DMSA caused an increase in semicircular diameter which could be attributed to an increase in electron-transfer resistance ($R_{ct,\ Au}$ = 15.6 kΩ; $R_{ct,\ Au/DMSA}$ = 47.2 kΩ). A smaller semicircular diameter of Au electrode indicates the faster electron-transfer kinetics of $Fe(CN)_6^{3-/4-}$ on bare gold surface [25]. In measurements with $Ru(NH_3)_3^{3+/2+}$ (Fig. 2b, inset), a decrease in R_{ct} was observed ($R_{ct,\ Au}$ = 6.3 kΩ; $R_{ct,\ Au/DMSA}$ = 3.1 kΩ), which can be ascribed to electrostatic attraction between negatively charged electrode surface and positive redox pair. Capacity values were falling for measurement with both redox probes (from 35.5 to 28.3 μF for $Fe(CN)_6^{3-/4-}$ and from 32.2 to 29.0 μF for $Ru(NH_3)_3^{3+/2+}$, which is in good agreement with the theory [26]. As expected, solution resistance and Warburg diffusion parameter are practically the same for both measurements setups. These results confirm those obtained with CV.

Characterization of Au and Au/DMSA electrodes in Cu^{2+} solution. Cyclic voltammograms of Au and Au/DMSA electrodes were recorded in 0.1 M ACB containing 0.1 M $NaClO_4$, pH 4.6, with 0.1 M $Cu(NO_3)_2 \cdot 3H_2O$. CV for Au (Fig. 3a) demonstrated two distinct waves at 27 (I$_a$) and 245 mV (II$_a$) at the anodic part of the voltammogram. Waves indicate two oxidation reactions. Wave I$_a$ corresponds to:

$$Cu \rightarrow Cu^+ + e^-, \qquad (1)$$

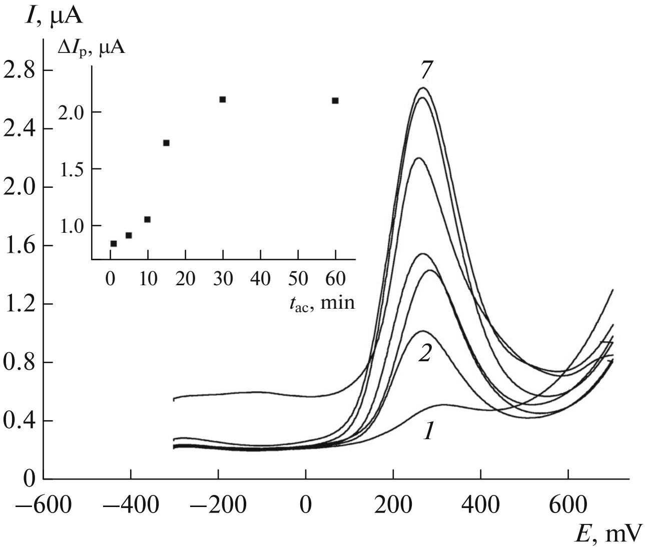

Fig. 4. AdTSV voltammograms of accumulation time influence on the electrode response. Accumulation was done in 2×10^{-5} M Cu–His, stripping was done in 0.1 M ACB containing 0.1 M $NaClO_4$, pH 4.6, reduction time 15 s, scan rate 20 mV/s, pulse height 25 mV, reduction potential –300 mV; supporting electrolyte (*1*), accumulation time 1 (*2*), 5 (*3*), 10 (*4*), 15 (*5*), 30 (*6*), and 60 min (*7*). Inset: anodic current (ΔI_p, μA) vs. accumulation time (t_{ac}, mV), where ΔI_p was calculated as $I_{Cu-His} - I_{supporting\ electrolyte}$.

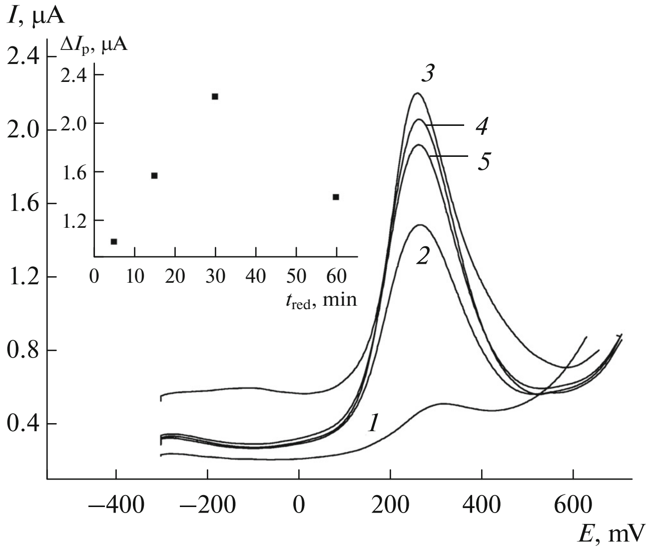

Fig. 5. AdTSV voltammograms of reduction time influence on the electrode response. Accumulation was done in 2×10^{-5} M Cu–His, stripping was done in 0.1 M ACB containing 0.1 M $NaClO_4$, pH 4.6, scan rate 20 mV/s, pulse height 25 mV, reduction potential –300 mV, accumulation time 15 min; supporting electrolyte (*1*), deposition time 5 (*2*), 15 (*3*), 30 (*4*) and with 60 s (*5*). Inset: anodic current (ΔI_p, μA) vs. deposition time (t_{red}, mV), where ΔI_p was calculated as $I_{Cu-His} - I_{supporting\ electrolyte}$.

while wave II_a describes:

$$Cu^{+} \rightarrow Cu^{2+} + e^{-}. \qquad (2)$$

In the cathodic part, a poorly visible peak at 181 mV (III_a) and one at –132 mV (IV_a) represent a two-step reduction from Cu^{2+} to Cu^0. CV of Au/DMSA electrode (Fig. 3b) demonstrated behavior different than Au. In general, the current values are significantly lower, since DMSA slowed the charge transfer reaction. At the anodic part of the voltammogram only one wave (I_b) at 280 mV was present. Considering the potential at which the wave is positioned it corresponds to the oxidation described by equation:

$$Cu \rightarrow Cu^{2+} + 2e^{-}. \qquad (3)$$

It is presumable that I_b represents two one-electron reactions integrated in one wave. Probable explanations for such behavior of modified electrode are a decrease in oxidation rate for Eq. (1) or a decrease between the oxidation potentials, as a result of which the two waves were integrated into one. On the cathodic part, two inadequately separated and poorly visible waves at 150 (II_b) and 12 mV (III_b) were observed corresponding to the reduction reactions.

Optimization. To investigate the capacity of Au/DMSA electrode for Cu–His binding, 2×10^{-5} M Cu–His complex solution was prepared. The influence of accumulation time, reduction time and reduction potential on the electrode response were examined. Measurements were carried out in the differential pulse mode of the stripping process. Accumulation of Cu–His on the modified surface was performed at open circuit potential by immersion Au/DMSA electrode in 10 mL of a stirred solution. After accumulation, the electrode was thoroughly rinsed and polarized at –300 mV. Polarization caused a reduction of Cu^{2+} from Cu–His, which was then anodically oxidized and the current response was measured. Complex on the electrode surface was formed primarily due to the electrostatic attraction between the deprotonated carboxylic groups of DMSA and positive Cu–His complex. Regeneration between measurements was completed by inserting thee modified electrode in stirred solution of 0.2 M EDTA for 3 min. After 3 min, a control AdTSV measurement was done (data not shown). It was found that there was no response; hence, it was concluded that EDTA complexed all of the remaining copper from the electrode. It is evident (Fig. 4) that maximum current response was achieved at the maximum accumulation time (60 min). With prolonged contact of Au/DMSA and Cu–His complex solution, the amount of electroactive substance increased on the surface of the modified electrode. Sixty minutes of accumulation time resulted in a minimal current increase, compared to 30 min, from which we could conclude that surface saturation was accomplished. In the subsequent measurements, accumulation time of 15 min was selected, since the

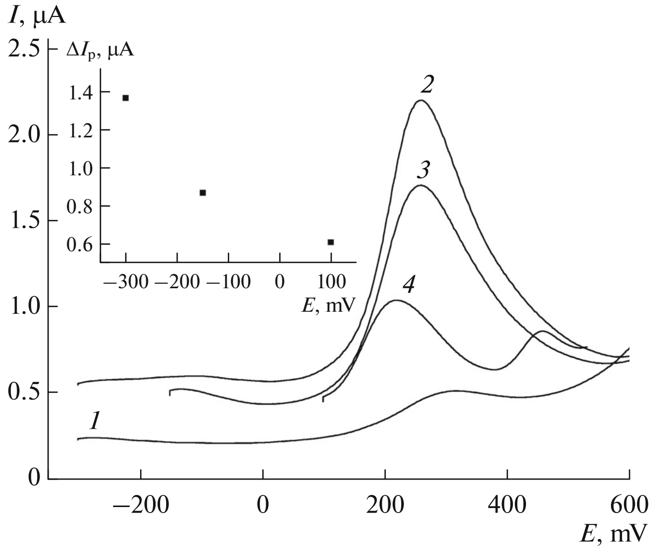

Fig. 6. AdTSV voltammograms of reduction potential's influence on the electrode response. Accumulation was done in 2×10^{-5} M Cu–His complex, stripping was done in 0.1 M ACB containing 0.1 M $NaClO_4$, pH 4.6, accumulation time 15 min, reduction time 15 s, scan rate 20 mV/s, pulse height 25 mV; supporting electrolyte (*1*) reduction potential –300 (*2*), –150 (*3*), +100 (*4*) mV. Inset: anodic current (ΔI_p, μA) vs. reduction potential (*E*, mV), where ΔI_p was calculated as $I_{Cu-His} - I_{supporting\ electrolyte}$.

response signal was analytically adequate and the waiting period for the formation of the complex was acceptable. Reduction time denotes the duration of polarization of the modified electrode with adsorbed complex at –300 mV. Four different reduction times were examined. It was found (Fig. 5) that the anodic current increases with increasing reduction time for 5, 15 and 30 s. Sixty seconds of reduction time caused a decrease in anodic current as a result of the significant loss of electroactive species from the surface of the Au/DMSA electrode. Reduction time of 15 s was chosen for further measurements, as the response signal was analytically sufficient and waiting period for the polarization of the electrode was acceptable.

The dependence of anodic current on the reduction potential was investigated. The decreasing trend in the response with increasing reduction potential was expected (Fig. 6). A higher reduction potential provided a smaller amount of copper, hence a decrease in the analytical signal was noticed. Maximum response was obtained for –300 mV of reduction potential, while the minimal signal was for +100 mV, which was expected, given the standard reduction potential of copper. The reduction potential of –300 mV was used in further experiments.

Voltammograms for pre-adsorbed Cu–His on the Au/DMSA were recorded under optimized conditions (Fig. 7). The dependence of the current response on the Cu–His concentration was linear in the range from 1×10^{-7} to 1×10^{-4} M (inset in Fig. 7). Linear relationship is given by equation:

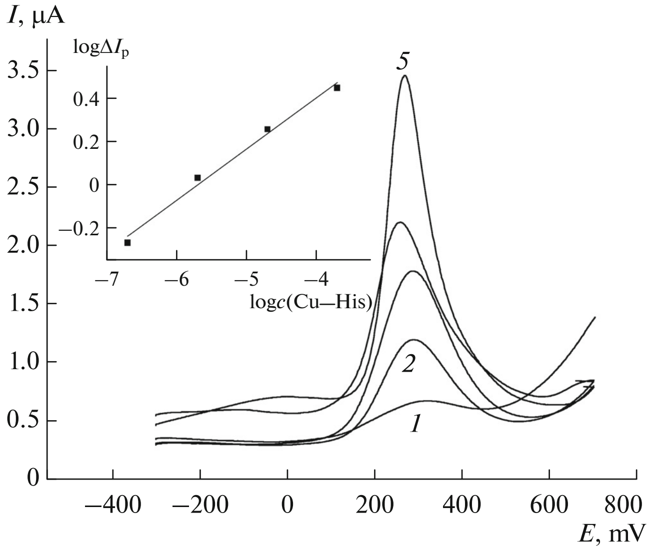

Fig. 7. AdTSV voltammograms of Cu–His concentration influence on the electrode response. Accumulation time 15 min, reduction time 15 s, reduction potential –300 mV, scan rate 20 mV/s, pulse height 25 mV, stripping was done in 0.1 M ACB containing 0.1 M $NaClO_4$, pH 4.6; supporting electrolyte (*1*), concentration of Cu–His 1×10^{-7} (*2*) to 1×10^{-4} (*5*) M. Inset: calibration graph.

$$\log \Delta I_p = (1.36 \pm 0.09) + (0.24 \pm 0.02) \log c(\text{Cu–His}), \quad R^2 = 0.9839.$$

***

This paper describes the surface modification of gold electrode and formation of Au/DMSA. With CV and EIS, the assembly of DMSA was examined. Results clearly demonstrate the existence of its layer on the electrode. After surface preparation, it was tested for Cu–His binding with AdTSV. The optimum working conditions, in which the designed electrode can perform, were determined. Since the prepared complex has a 1 : 1 composition, the measured concentration of copper was equivalent to concentration of His. The sensor demonstrated a linear relationship of $\log \Delta I_p$ on logc(Cu–His) in the range from 1×10^{-7} to 1×10^{-4} M.

ACKNOWLEDGMENTS

We are grateful to the Croatian Ministry of Science, Education and Sports for the financial support of the study.

REFERENCES

1. Nuzzo, R.G. and Allara, D.L., *J. Am. Chem. Soc.*, 1983, vol. 105, p. 4481.

2. Love, J.C., Estroff, L.A., Kriebel, J.K., Nuzzo, R.G., and Whitesides, G.M., *Chem. Rev.*, 2005, vol. 105, p. 1103.
3. Kopple, J.D. and Swendseid, M.E., *J. Clin. Invest.*, 1975, vol. 55, p. 881.
4. Stifel, F.B. and Herman, R.H., *Am. J. Clin. Nutr.,* 1971, vol. 24, p. 207.
5. Liedberg, B., Carlsson, C., and Lundström, I., *J. Colloid Interface Sci.*, 1987, vol. 120, p. 64.
6. Marti, E.M., Quash, A., Methivier, C., Dubot, P., and Pradier, C.M., *Colloids Surf.*, A, 2004, vol. 249, p. 85.
7. Deschamps, P., Kulkarni, P.P., Gautam-Basak, M., and Sarkar, B., *Coord. Chem. Rev.*, 2005, vol. 249, p. 895.
8. Krogh-Jespersen, K., Westbrook, J.D., Potenza, J.A., and Schugar, H.J., *J. Am. Chem. Soc.*, 1987, vol. 109, p. 7025.
9. Evertsson, B., *Acta Crystallogr., Sect. B*, 1969, vol. 25, p. 30.
10. Baidina, I., Slyudkin, O., and Borisov, S., *J. Struct. Chem.*, 1990, vol. 31, p. 503.
11. Czernuszewicz, R.S., Yan, Q., Bond, M.R., and Carrano, C.J., *Inorg. Chem.*, 1994, vol. 33, p. 6116.
12. Perrin, D.D. and Sharma, V.S., *J. Chem. Soc. A,* 1967, p. 724.
13. Bersuker, I.B., *Coord. Chem. Rev.*, 1975, vol. 14, p. 357.
14. Murphy, B. and Hathaway, B., *Coord. Chem. Rev.*, 2003, vol. 243, p. 237.
15. Shervedani, R.K., Mehrjardi, A.H., and Zamiri, N., *Bioelectrochemistry*, 2006, vol. 69, p. 201.
16. Palecek, E., *Bioelectrochem. Bioenerg.*, 1992, vol. 28, p. 71.
17. Aiba, H., Yokoyama, A., and Tanaka, H., *Bull. Chem. Soc. Jpn.*, 1974, vol. 47, p. 1003.
18. Crisponi, G., Cristiani, F., Nurchi, V.M., Pinna, R., Pivetta, T., José Tapia Estévez, M., *Polyhedron*, 2000, vol. 19, p. 2435.
19. Sabatani, E., Rubinstein, I., Maoz, R., and Sagiv, J., *J. Electroanal. Chem.*, 1987, vol. 219, p. 365.
20. Kissinger, P.T. and Heinman, W.R., J. *Chem. Educ.*, 1983, vol. 60, p. 702.
21. Amatore, C., Savéant, J.M., and Tessier, D., J. *Electroanal. Chem.*, 1983, vol. 147, p. 39.
22. Finklea, H.O., Snider, D.A., Fedyk, J., Sabatani, E., Gafni, Y., and Rubinstein, I., *Langmuir*, 1993, vol. 9, p. 3660.
23. Macdonald, J.R. and Johnson, W.B., in *Fundamentals of Impedance Spectroscopy*, Barsoukov, E. and Macdonald, J.R., Eds., New Jersey: Wiley, 2005, p. 2.
24. Yang, L.J. and Li, Y.B., *Biosens. Bioelectron.*, 2005, vol. 20, p. 1407.
25. Yang, Y.J. and Khoo, S.B., *Sens. Actuators*, B, 2004, vol. 97, p. 221.
26. Katz, E. and Willner, I., *Electroanalysis*, 2003, vol. 15, p. 913.